Available online at www.sciencedirect.com
ScienceDirect
Thermochimica Acta 455 (2007) 55–59
thermochimica acta
www.elsevier.com/locate/tca

Measurement of the thermal conductivity of TiO_2 thin films by using the thermo-reflectance method

Jungho Mun [a], Sok Won Kim [a,*], Ryozo Kato [b], Ichiro Hatta [c], Sang Hyun Lee [d], Kweon Ho Kang [e]

[a] *Department of Physics, University of Ulsan, Ulsan 680-749, Republic of Korea*
[b] *Ulvac-Riko Inc., Hakusan, Midoriku, Yokohama 226, Japan*
[c] *Fukui University of Technology, 3-6-1 Gakuen, Fukui 910-0028, Japan*
[d] *Division of Physical Metrology, Korea Research Institute of Standards and Science, Daejon 305-600, Republic of Korea*
[e] *Korea Atomic Energy Research Institute, P.O. Box 105, Yusong, Daejon 305-600, Republic of Korea*

Available online 30 November 2006

Abstract

The through-plane thermal conductivity of TiO_2 thin films, with the thicknesses of 150 and 300 nm, deposited on silicon wafers and heat treated at several different temperatures was measured using the thermo-reflectance method which utilizes the reflectance variation of the films surface produced by the periodic temperature variation. The results showed that the thermal conductivities were 0.7–1.7 $W\,m^{-1}\,K^{-1}$ and increase as the heat treatment temperature increases. They are explained by the grain size and the density of the heat treated films. Also the thermal conductivity of 300 nm thick film is larger than that of 150 nm thick film by 30%. The reason for that was assumed to be the thermal resistance between the thin film, metal film and the substrate.
© 2006 Elsevier B.V. All rights reserved.

Keywords: Thermo-reflectance method; Thermal conductivity; TiO_2 thin film; Heat treatment

1. Introduction

The device characteristics of micro-electronic system can be changed largely by the heat generated in the circuit. Therefore, the thermal conductivity measurement technique of electrically insulated thin film has been required to estimate the heat dissipation from the thin film components to the circuit board composed by silicon wafers.

There are many kinds of thermal conductivity measurement method of thin films. However, since advanced thin films are newly composed and their thickness becomes thinner, the existing methods have limitations and new methods have been required. One of them is pico-second thermo-reflectance method developed by Taketoshi et al., for the measurement of the through-plane thermal conductivity of thin films coated on the substrate [1]. In this method the bottom surface of the thin film is heated by laser-flash lighter, which is transferred through the substrate, and the temperature response of the top surface is measured. However, this method is not applicable to low-thermal conductivity thin films coated on a high thermal conductivity substrate.

In order to measure the through-plane thermal conductivity of very thin films coated on a substrate, the 3ω (three-omega) method has been developed by Lee and Cahill, and applied well to the various electrically insulating thin films [2]. However, the 3ω method has a disadvantage in that a fine pattern of the metal film must be deposited on the thin film sample surface, because the method is based on a two-dimensional thermal conductivity measurement system [3].

In this study, the through-plane thermal conductivity of TiO_2 thin films coated on the silicon wafer was measured by using the thermo-reflectance method, developed by Kato and Hatta [4]. In this method, a wide metal film, which is deposited on the thin insulating films, is Joule heated periodically and the ac-temperature response at the center of the metal film surface is measured by the variation of reflectance because it depends on the ac-temperature response of the metal film surface. Thus, the one-dimensional model of the thermal conduction equation can be applied for the three-layered system.

* Corresponding author. Tel.: +82 52 259 2388; fax: +82 52 259 1693.
E-mail address: sokkim@ulsan.ac.kr (S.W. Kim).

0040-6031/$ – see front matter © 2006 Elsevier B.V. All rights reserved.
doi:10.1016/j.tca.2006.11.018

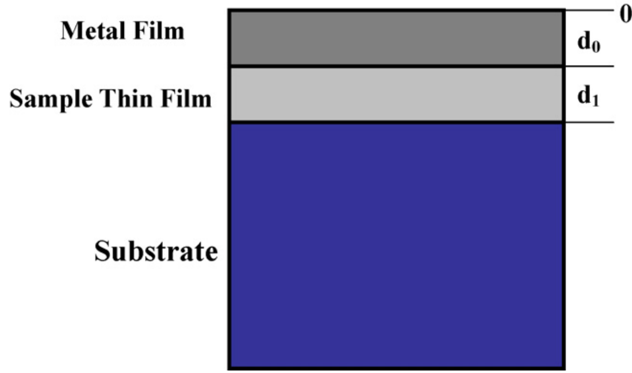

Fig. 1. Schematic diagram of the sample geometry used for the thermal conductivity measurements.

The TiO_2 thin films have attracted great attention for electrodes, chemical sensors, ceramic membranes, and of course as a photo-catalyst. In particular, transparent TiO_2 thin film photocatalysts are expected to have wide applications for elimination of environmental pollutants [5]. On the other hand, control of the film morphology is of interest for increasing the electrochemical or photo-catalytic property of thin films [6].

2. Theoretical background

Fig. 1 shows the schematic diagram of the thermal conductivity measurement system. As shown in Fig. 1, it consists of three layers, the metal film layer, the thin-film layer, and the layer of substrate. In the system, when the metal film is Joule heated periodically with the frequency of ω, the ac-temperature of the metal film surface varied with the frequency of 2ω and a small temperature excursion (ΔT) about average temperature T, can be related linearly to a fractional change (ΔR) in reflectance of the surface as follow [7];

$$\frac{\Delta R}{R} = C(\lambda)\frac{\Delta T}{T} \tag{1}$$

where R is the surface reflectance, and $C(\lambda)$ is the coefficient of reflectance-temperature and depends on prove wavelength.

Although the metal film is ac-heated uniformly, an ac-temperature gradient along the thickness of the metal film layer may take place. It is assumed in the system that the substrate layer has infinite thickness, but the metal film layer and the thin film layer have finite thickness. The one-dimensional thermal conduction equation of the system in the through-plane direction was solved analytically and next equation shows the surface temperature [4].

$$T(0) = \frac{q}{i\omega C_0}\left\{1 + \left(\frac{((\lambda_0 k_0/\lambda_s k_s) - (\lambda_0 k_0/\lambda_1 k_1))\exp[-(1+i)k_1 d_1]\sinh[(1+i)k_0 d_0]}{\lambda_1 k_1/\lambda_s k_s \sinh[-(1+i)k_1 d_1] - \cosh[-(1+i)k_1 d_1]} - \cosh[(1+i)k_0 d_0] - \frac{\lambda_0 k_0}{\lambda_1 k_1}\sinh[(1+i)k_0 d_0]\right)^{-1}\right\} \tag{2}$$

where q denotes the heat per unit volume, d_i, k_i and λ_i denote the thickness of the layer, thermal-wave number in the layer, and thermal conductivity of that layer, respectively(s, 1, and 0 denotes the substrate, sample film, and metal film, respectively).

When the fallowing conditions are valid,

$$k_0 d_0 \ll 1 \tag{3a}$$

$$k_1 d_1 \ll 1 \tag{3b}$$

Eq. (2) can be simplified to the following equation:

$$\frac{T_0}{qd_0} = \frac{\exp(-(\pi/4)i)}{\sqrt{\lambda_s C_s \omega}} + \left(1 - \sqrt{\frac{\lambda_1 C_1}{\lambda_s C_s}}\right)\frac{d_1}{\lambda_1} + \left(\frac{1}{2} - \frac{\lambda_0 C_0}{\lambda_s C_s}\right)\frac{d_0}{\lambda_0} \tag{4}$$

The first term of the right-hand side of Eq. (4) is proportional to $\omega^{-1/2}$. On the other hand, the second and third terms of Eq. (4) are real constants independent of $\omega^{-1/2}$. The plot of $T(0)/qd_0$ versus $\omega^{-1/2}$ gives the slope and the interception point. So the thermal effusivity of the substrate $\lambda_s C_s$ can be determined from the slope, and the sum of the second and third terms can be determined from the interception point. To determine an absolute value of the thermal conductivity of a thin film, the calibration factor of the thermo-reflectance coefficient must be known. However, it is very difficult to make a calibration using conventional temperature standards, because the thermo-reflectance coefficients of metals are generally very low. Therefore, in this study, coefficient of reflectance-temperature is determined by using the proportionality factor obtained by dividing the experimental slope with the theoretical slope of the graph.

Assuming that the thermal effusivity of the metal film $\lambda_0 C_0$ is much smaller than that of the substrate $\lambda_s C_s$, the third term of Eq. (4) is reduced to half of the thermal resistance of the metal film. Assuming that the thermal effusivity of the thin film $\lambda_1 C_1$ is much smaller than that of the substrate $\lambda_s C_s$, the second term of Eq. (4) is reduced to the thermal resistance of the thin film.

The value of the third term of Eq. (4) can be determined theoretically using the known values of d_0, λ_0, C_0, λ_s, and C_s. The value of the second term of Eq. (4) can be determined by subtracting the theoretically obtained value of the third term from the experimentally obtained value of the sum of the second and third terms.

The following equation, which is a quadratic equation of $\lambda^{-1/2}$, is given by defining the second term of Eq. (4) as R_1^*;

$$R_1^* = \left(1 - \sqrt{\frac{\lambda_1 C_1}{\lambda_s C_s}}\right)\frac{d_1}{\lambda_1} \tag{5}$$

The solution of Eq. (5) is given by the following equation;

$$\sqrt{\frac{1}{\lambda_1}} = \sqrt{\frac{R_1{}^*}{d_1} + \frac{C_1}{4\lambda_s C_s}} + \sqrt{\frac{C_1}{4\lambda_s C_s}} \tag{6}$$

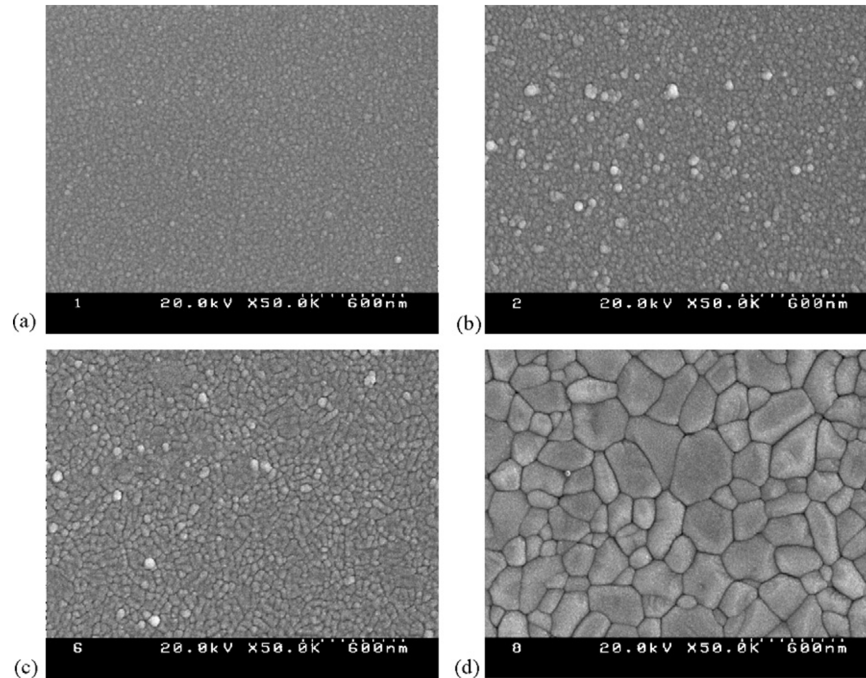

Fig. 2. Microphotographs of TiO_2 thin films (a) as-prepared; (b) heat treated at 300 °C; (c) heat treated at 600 °C; and (d) heat treated at 900 °C.

Finally, by substituting the experimentally obtained value of R_1^* into Eq. (6) and using the known values of d_1, C_1, λ_s, and C_s, the thermal conductivity of the thin film λ_1 can be determined.

3. Experimental

3.1. Sample preparation

The TiO_2 thin film samples were prepared by RF sputtering. The 0.6 mm silicon wafers, rinsed with ultra-pure water, ethanol, and acetone, were used as substrates after the blowing off the dusts and moisture on the wafer surface. Before the deposition, the sputtering target is fabricated by the compression of TiO_2 powders with high pressure and sintered in high temperature. The initial pressure of the vacuum chamber was less than 4×10^{-6} Torr and the pre-sputtering was performed for 5 min at a pressure of 4×10^{-2} Torr to remove the impurities and oxidation layers on the target.

During the deposition, the temperature of the substrate and the pressure of the Ar gas were maintained to 230 °C and 1×10^{-2} Torr, respectively. The 200 W RF power was applied to the target and the distance between the substrate and target was maintained as 15 cm, and the substrate rotates with 5 rpm. The deposition thicknesses of the films were 150 and 300 nm, and their times were 1.5 and 3 h, respectively. After the deposition, the samples were heat-treated for 1 h at 300, 600, and 900 °C.

Fig. 2 shows the microphotograph of four kinds of samples (one is not heat-treated and another three are heat-treated). The grain size of not heat-treated sample is very small however, those of heat-treated samples at 300 °C and 600 °C partly and fully increase to 30 μm, respectively, and the grain size at 900 °C becomes to 100 μm. From this result, we can find that the grain size of the sample surface is strongly depends on the heat-treatment temperature.

3.2. Thermal conductivity measurement

Fig. 3 is a top-view of the block diagram of the experimental setup. The thermo-electric cooler system keeps the sample stage at a constant temperature (25 °C). The whole system assembly is installed in a vacuum chamber to prevent the convection and

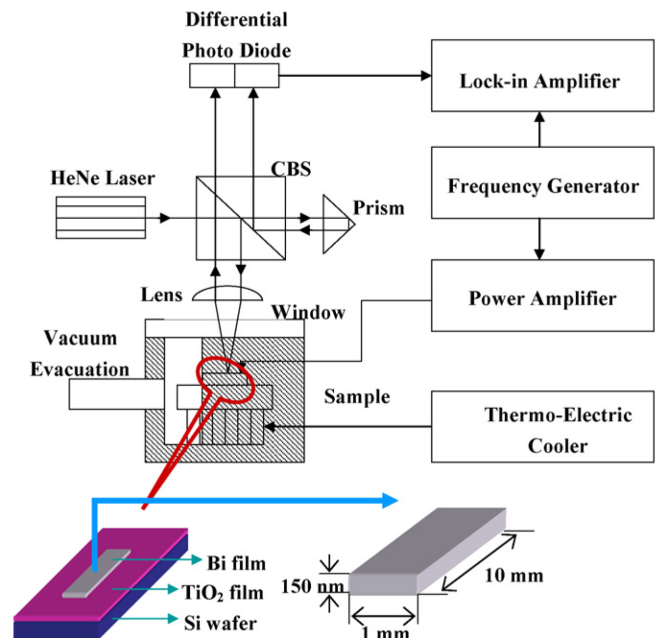

Fig. 3. Block diagram of the experimental setup. The specimen is set vertically on the sample stage.

Table 1
Thicknesses and thermophysical properties of materials used in the present study

Materials	Thickness	Thermal conductivity ($W m^{-1} K^{-1}$)	Specific heat capacity per unit volume ($J cm^{-3} K^{-1}$)
Silicon wafer	0.6 mm	148 (λ_s)	1.66 (C_s)
Bismuth film	150 nm	1.46 (λ_0)	1.19 (C_0)
TiO_2 film	150 nm, 300 nm (d_1)		0.55 (C_1)

oxidation. At the front of the chamber, an optical window is provided to enable thermo-reflectance measurement. The size of the sample is 25 mm × 12.5 mm. The bismuth metal film with the thickness of 150 nm is deposited on the sample film by evaporation with a mask made of stainless steel foil because the temperature coefficient of bismuth film is about 900 ppm K^{-1} and it is quite large compared to other metal films such as gold of 30 ppm K^{-1} [4]. At both ends of the metal film, a pair of electrodes made of silver paste is printed for supplying ac-current and detecting ac-voltage.

One of the two-divided He–Ne laser beams by the cubic beam splitter is reflected from the sample surface and the other one is reflected from the prism, and both of them go into the differential photodiode. As the frequency of the ac-current (ω) changes, the variation of the reflectance of sample surface is measured by the lock-in amplifier (Stanford, SR 830). The sine output signal from the frequency generator (HP8116A) is amplified by the power amplifier to energize the metal film deposited on the sample film. The differential photodiode is plugged into the current input port of the lock-in amplifier to measure the second harmonic of the photocurrent signal.

4. Results and discussion

The sample condition and the thermophysical properties used in the calculation in Eqs. (4)–(6) are listed in Table 1 [8,9]. Fig. 4(a) and (b) are the average values of the signals, measured for five times and corrected by Eq. (1), plotted for $\omega^{-1/2}$ from the four kinds of samples for each thicknesses of 150 and 300 nm TiO_2 film samples deposited on silicon, respectively, in the frequency range from 2000 to 10,000 Hz. In this case, the average value of the correction factor was determined as 3.25×10^{-4} by using the thermal effusivity of silicon wafer. As predicted in Eq. (4), the plot shows good linearity in the measurement frequency ranges.

Except the value of interception points, Fig. 4(a) and (b) show almost the same trends. The apparent thermal resistance R_1^* was obtained by subtraction the theoretically obtained third term of Eq. (4) from the experimental results of the interception points. By substituting R_1^* and the values in Table 1 into Eq. (6), the thermal conductivity of TiO_2 thin film was obtained.

The interception points and the obtained thermal conductivity values are listed in Table 2. From this, we can find that the obtained thermal conductivity is in the range from 0.7 to 1.7 $W m^{-1} K^{-1}$ and it agrees well with the literature values obtained by 3ω method [10]. Also it shows that as the temperature of heat treatment increases, the thermal conductivity increases because the thermal resistance proportional to the number of heat transfer interfaces decreases as the grain size of the film becomes large in higher heat-treatment temperatures as shown in Fig. 2. The grain size of the sample heat-treated at 900 °C became quite larger compared to the case of 300 °C and 600 °C, however, the increment of the thermal conductivity is relatively smaller because of the density reduction of the film material caused by the increment of grain size. For the more detail investigation, the more precise data for the variation of density is required. The uncertainty in the thermal conductivity measurement was ± 8.5% and it obtained by the variation of the interception values for the five measurements.

The result also shows that the thermal conductivity of two time thicker films is larger than thinner films about 30%. This can be explained by the effect from the thermal resistances between the metal film, sample film, and the surface of silicon substrate. If we assume that these resistances exist, the obtained film thermal

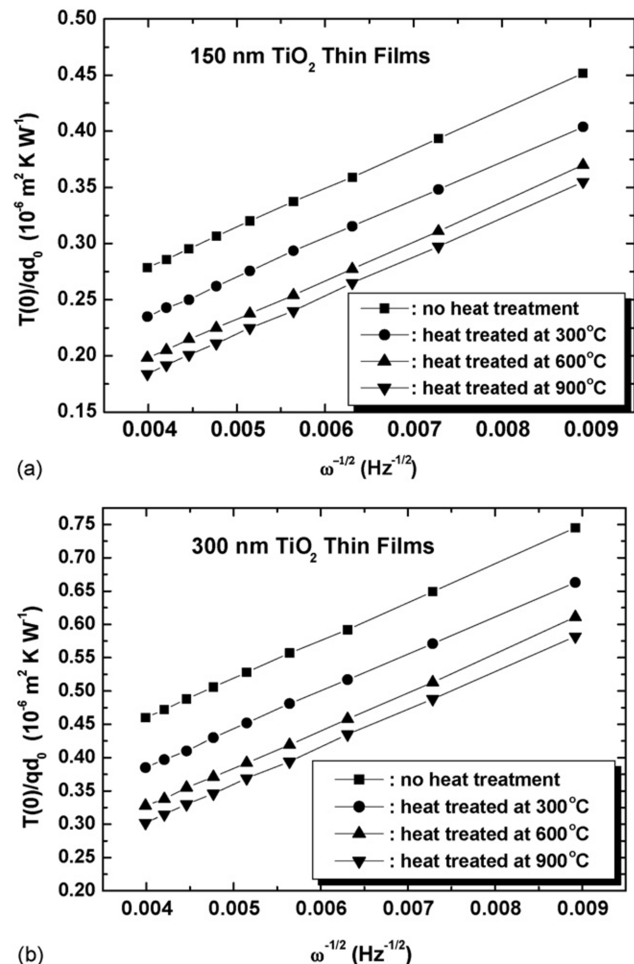

Fig. 4. $T(0)/qd_0$ vs. $\omega^{-1/2}$ plot for thermal conductivity measurement of the TiO_2 thin films with (a) thickness of 150 nm and (b) thickness of 300 nm.

Table 2
The obtained thermal conductivity by the measurement of the interception point of the linearly fitted line and the vertical-axis

Thickness	Thin film samples	Interception point (10^{-6} m^2 K W^{-1})	Thermal conductivity (W m^{-1} K^{-1})
	No heat-treatment	0.262	0.70 ± 0.06
150 nm	Heat treated at 300 °C	0.217	0.90 ± 0.07
	Heat treated at 600 °C	0.181	1.15 ± 0.10
	Heat treated at 900 °C	0.169	1.27 ± 0.10
	No heat-treatment	0.426	0.92 ± 0.07
300 nm	Heat treated at 300 °C	0.357	1.17 ± 0.08
	Heat treated at 600 °C	0.302	1.49 ± 0.12
	Heat treated at 900 °C	0.281	1.68 ± 0.14

conductivity λ_1 can be expressed as $\lambda_1 = \lambda_i/(1+\lambda_i R_i/d_i)$, where λ_i is the intrinsic thermal conductivity of thin film independent to the thickness of film, and R_i is the total thermal resistance between the layers. According to this expression, we can see that the experimentally obtained thermal conductivity λ_1 is always lower than λ_i and thinner films show lower λ_1 than thicker film. Actually, because the thermal resistance R_i of the amorphous film is in 2–4 × 10^{-8} m^2 K W^{-1} [11] depending the thickness, the thermal conductivity changes about 20–30% at maximum, therefore for the additional accurate investigations, the real thermal resistance of sample film, substrate, and metal film should be required.

5. Conclusions

By using the thermo-reflectance method which utilizes the reflectance variation of the films surface produced by the periodic temperature variation, the through-plane thermal conductivity of TiO_2 thin films, with the thicknesses of 150 nm and 300 nm, deposited on silicon wafers and heat treated at several different temperatures were measured. The results showed that the thermal conductivities were 0.7–1.7 W m^{-1} K^{-1} and increase as the heat treatment temperature increases, and could be explained by relations with the grain size and the density of the heat treated films. Also the thermal conductivity of 300 nm thick film is larger than that of 150 nm thick film by 30% and the reason for that was explained by the thermal resistance between the thin film, metal film and the substrate. This result will be applied to the electronic circuits which utilize the thermal properties of the functional thin films.

Acknowledgment

This work was supported by the Ministry of Commerce, Industry and Energy (MOCIE) of the Republic of Korea, through the Research Center for Machine Parts and Materials Processing (ReMM) at the University of Ulsan.

References

[1] N. Taketoshi, T. Baba, A. Ono, Jpn. J. Appl. Phys. 38 (1999) L126.
[2] S.-M. Lee, D.G. Cahill, Phys. Rev. B52 (1995) 253.
[3] S.-M. Lee, D.G. Cahill, J. Appl. Phys. 81 (1997) 2590.
[4] R. Kato, I. Hatta, Proceedings of the 23rd Jpn. Symp. Thermophys. Prop., 2000, pp. 10–12.
[5] N. Negishi, K. Takeuchi, Mater. Lett. 38 (1999) 150.
[6] S.W. Ryu, E.J. Kim, S.K. Ko, S.H. Hahn, Mater. Lett. 58 (2004) 582.
[7] D. Guidotti, H.M. van Driel, Appl. Phys. Lett. 47 (1985) 1336.
[8] Thermophysical Properties Handbook, Japanese Thermophysical Society, Yukendo, Ltd., 1990, pp. 18–33.
[9] D.M. Zhu, T. Kosugi, J. Non-Cryst. Solids 202 (1996) 88.
[10] D.J. Kim, D.S. Kim, S. Cho, S.W. Kim, S.H. Lee, J.C. Kim, Int. J. Thermophys. 25 (2004) 281.
[11] T. Yamane, N. Nagai, S. Katayama, M. Todoki, J. Appl. Phys. 91 (2002) 9772.